Hindawi
Journal of Nanomaterials
Volume 2022, Article ID 5005148, 9 pages
https://doi.org/10.1155/2022/5005148

Research Article

Cotton Fabric Dyed with Self-Dispersive and Reactive Nanocarbon Black for Enhanced Static Resistance and UV Protection

Zhenming Qi,[1] Wenhui Yu,[1,2] Jialong Tian,[1,3] Kuang Wang,[1,2,4] Jiayi Chen,[1] Dawei Gao,[1] Yu Ren,[1,2] and Chunxia Wang [1,2,3]

[1]*College of Textile and Clothing, Yancheng Institute of Technology, Jiangsu 224051, China*
[2]*School of Textile and Clothing, Nantong University, Jiangsu 226019, China*
[3]*School of Textile Science and Engineering, Xi'an Polytechnic University, Shanxi 710048, China*
[4]*College of Textile Science and Engineering, Jiangnan University, Jiangsu 214122, China*

Correspondence should be addressed to Chunxia Wang; cxwang@mail.dhu.edu.cn

Received 7 August 2021; Revised 14 November 2021; Accepted 25 November 2021; Published 18 January 2022

Academic Editor: Mazeyar Parvinzadeh Gashti

Amino functionalized nanocarbon black (CB/KH550) was prepared in reaction between KH550 and nanocarbon black (CB). 2-(4-(4,6-dichloro-1,3,5-triazin-2-ylamino)phenylsulfonyl)ethyl) sodium sulfate (SDTES) was synthesized and characterized. Self-dispersive and reactive nanocarbon black (CB/KH550/SDTES) was prepared by nucleophile substitution reaction and characterized by FTIR, TEM, zeta potential, and TG analysis. Cotton fabric was dyed with CB/KH550/SDTES by dip-dyeing method and was observed by SEM. Moreover, color depth, static resistance, UV protection, tensile property, and rub fastness of cotton fabric were measured and analyzed. Results showed that CB/KH550/SDTES demonstrated excellent dispersion stability. The dyed cotton fabric possessed adorable antiultraviolet and antistatic properties. The preparation mechanism of the cotton fabric dyed with CB/KH550/SDTES was proposed.

1. Introduction

Black hue is regarded as the one of most classic color in fashion, and black clothes have dominated the wardrobe for centuries, where black dyes have emerged and been developed since then [1–5]. Black dyes were primarily obtained from benzidine-derived azo, which showed good dyeability and fixation rates. However, carcinogenic intermediates generated from manufacturing have prevented the black dyes from further application in the textiles and fashion industry. In recent years, nanocarbon black (CB) has drawn considerable attention due to its abundant resources, low cost, high blackness as well as excellent conductivity, dyeability, and chemistry stability [6, 7]. It is considered as an ideal candidate in textile printing and dyeing, batteries, rubber and plastics, and so on [8, 9]. Nevertheless, CB has poor dispersion in liquid medium, and the suspensions are prone to aggregate owing to its small particle size, large specific surface area, high surface energy, strong hydrophobicity, and van der Waals force between the particle [10–12]. Moreover, there exist a few polar and nonpolar groups on the surface of the particles which make it difficult to bond firmly with the fiber [13–15].

Some researchers urgently hope to improve the dispersibility and reactivity of CB through some strategies, including dispersant and polymer modification [16, 17]. Between them, the dispersant modification is to improve the dispersibility by adding certain dispersant to CB. This procedure is regarded as a simple and convenient method and does not cost much, but the dispersant is susceptible to fall off the textile surface [18–20]. The polymer modification is mainly to graft water-

soluble and reactive groups on the surface of CB. The water-soluble groups usually introduce steric hindrance and electrostatic effect to enhance the dispersibility of CB. And the reactive groups promote the fabric reaction to enhance the binding fastness between CB and the textile [21]. Li et al. fabricated a type of alkyl-carbon black nanoparticles with hydrophobic and lipophilic properties, and the obtained sample exhibited excellent dispersion ability in organic solutions [22]. Jiang et al. prepared aqueous phase self-dispersed CB composites by KH570-modifed CB and p-styrene sulfonate sodium through in-situ polymerization, and the composites showed excellent self-dispersibility in aqueous phase without extra treatment [23].

Therefore, in this paper, CB/KH550/SDTES would be prepared and applied to dye cotton fabric to enhance color depth, ultraviolet protection, and antistatic electricity. Meanwhile, the mechanism and reactions of CB/KH550/SDTES with cotton fabric would be explored.

2. Experimental

2.1. Materials. CB (MA100, industrial grade) was purchased from Shanghai Kaine Chemical Co., Ltd. 3-aminopropyltriethoxysilane (KH550, ≥98%), and acetone (AR) and ammonia solution (25%, AR) were provided by Jiangsu Tongsheng Chemical Reagent Co., Ltd. Cyanuric trichloride (AR) was supplied by Shanghai Aladdin Bio-Chem Technology Co., Ltd. Para-ester ($C_8H_{11}NO_6S_2$, industrial grade) was received from Suzhou Jiayet Bio Co., Ltd. Anhydrous sodium carbonate (Na_2CO_3, AR) was provided by Tianjin Dasheng Chemical Reagent Co., Ltd. Absolute ethanol (AR) and anhydrous methanol (AR) were obtained from Sinopharm Chemical Reagent Co., Ltd.

2.2. Preparation of Amino-Functionalized CB. In a typical procedure [24], KH550 (2.5 g) and $NH_3{\cdot}H_2O$ (0.5 mL) were dissolved in 90% aqueous ethanol (100 g). CB (5 g) was added to the solution accompanying with ultrasonic for 60 min. Afterward, the suspension was kept stirring vigorously at 40°C for 20 h. The precipitate was centrifuged and rinsed by absolute ethanol three times. Finally, the amino-functionalized CB (CB/KH550) was obtained after being dried at 60°C for 12 h and pulverized.

2.3. Synthesis of 2-(4-(4,6-Dichloro-1,3,5-Triazin-2-Ylamino)Phenylsulfonyl)Ethyl) Sodium Sulfate (SDTES). Para-ester (4.26 g) was dispersed in deionized water (12 mL), and Na_2CO_3 solution (4.4 mL) was added dropwise into the above solution under vigorous stirring at 0°C. Thereafter, the reaction was carried out for 40 min to achieve a greyish white suspension. Cyanuric chloride (2.85 g) was dispersed in deionized water (12 mL) and stirred for 30 min at 0°C to obtain transparent solution. The abovementioned off-white suspension and transparent solution were mixed together under continuous stirring for 30 min at 0°C, and the pH value of the mixture was adjusted to 3 ~ 4 by adding Na_2CO_3 solution (4 mL). Subsequently, the white suspension was acquired after reaction for 4 h. The product was salted out with saturated NaCl solution, filtrated, washed, and then filtrated with absolute ethanol and absolute methanol to remove unreacted cyanuric chloride and hydrolysis products, respectively. Finally, the product was dried in vacuum oven at 60°C to obtain SDTES off-white powder [25].

The structure and component of SDTES were investigated by Qone-WNMR-I-AS400 Nuclear magnetic resonance spectrometer (Q.One Instruments, China) and NEXUS-670 Fourier transform infrared spectrometer (NICOLET, America).

2.4. Preparation of Self-Dispersive and Reactive CB. SDTES (0.79 g) and CB/KH550 (0.5 g) were consecutively dispersed in acetone (20 mL). Na_2CO_3 solution was slowly added to adjust the pH to 5 ~ 6, followed by continuous stirring for 3 h at 40°C. The precipitate was centrifuged to remove the additional acetone, washed and centrifuged three times by the mixed solution of absolute methanol and absolute ethanol, and dried at 50°C. The self-dispersive and reactive CB/KH550/SDTES was obtained. The schematic diagram of CB/KH550/SDTES preparation is illustrated in Figure 1.

2.5. Characterization of CB and CB/KH550/SDTES. The infrared transmission spectra were investigated by NEXUS-670 Fourier transform infrared spectrometer (NICOLET, America). The JEM-1400 plus transmission electron microscope (Nippon Electronics, Japan) was performed to observe the morphology. Zetasizer nano-zs laser particle size analyzer (Malvern, England) was applied to determine the particle size, polymer dispersity index (PDI), and zeta potential. The sample was ultrasonically dispersed in deionized water for 30 min to form a uniform dispersion, which was observed before and after standing for one month. Q5000 heat loss analyzer (TA, America) was selected to characterize the thermal property.

2.6. Dyeing of Cotton Fabric by CB/KH550/SDTES. CB/KH550/SDTES (0.1 g) was added into deionized water (20 mL) and sonically vibrated for 30 min to achieve an evenly dispersed suspension. Then, NaCl (0.05 g), Na_2CO_3 (0.3 g), and cotton fabric (1 g) were added to the above suspension, which were oscillated for 40 min at 90°C. Subsequently, the cotton fabric dyed with CB/KH550/SDTES was obtained after being washed and dried.

The surface morphology of cotton fabric was observed by JSM-6700F field emission scanning electron microscope (JEOL, Japan).

2.7. Property Measurement of Cotton Fabric. Half-life of electrostatic voltage ($t_{1/2}$), volume-specific resistance (R_v), and surface specific resistance (Rs) were measured to evaluate the antistatic property of cotton fabric by YG(B)324E fabric inductive electrostatic tester (Wenzhou Darong Textile Instrument Co., Ltd, China) and ZC36 High Insulation Resistance Meter (Shanghai Anbiao Electronic Co., Ltd, China), respectively.

YG (B) 912E textile UV performance tester was applied to characterize the ultraviolet protection of cotton fabric.

The color depth was evaluated by Color-Eye 7000A computer color difference meter (X-Rite, America).

The fabric tensile tester (Shanghai Experimental Instrument Co. Ltd, China) and abrasive resistance tester (Jintan Medical Instrument Co. Ltd, China) were employed to study the tensile property and abrasive resistance of cotton fabric, separately.

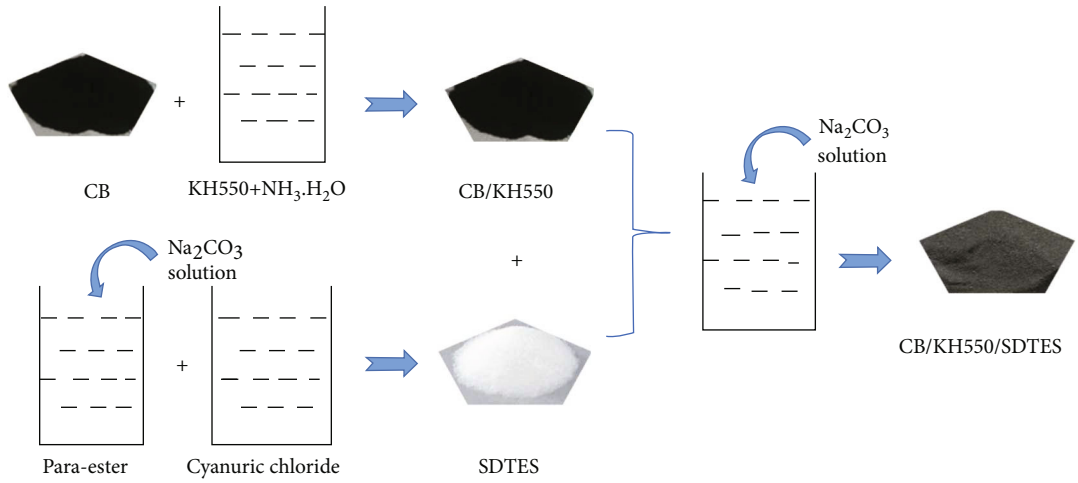

Figure 1: Schematic diagram of CB/KH550/SDTES preparation.

3. Results and Discussion

3.1. ^1H NMR Analysis. Figure 2 presents the ^1H NMR spectrum of SDTES. The data was as follows: ^1H NMR (400 MHz, DMSO) δ 11.60 (s, 1H), 7.93-7.86 (m, 4H), 3.94 (t, $J = 6.4$ Hz, 2H), and 3.61 (t, $J = 6.8$ Hz, 2H). It could be deduced that that SDTES was successfully synthesized.

3.2. FTIR Analysis. Figure 3 displays the FTIR spectrum of para-ester, cyanuric chloride, SDTES, CB, CB/KH550, and CB/KH550/SDTES. As shown in Figure 3(a), the absorption peak of SDTES at 3531 cm^{-1} was associated with the N-H stretching vibration on primary amine of the para-ester. The absorption peak at 3309 cm^{-1} indicated the vibration on the amino group of SDTES. The absorption peak at 2918 cm^{-1} matched well with the absorption peak on the methylene group of SDTES. The absorption peaks at 1537~1287 cm^{-1} indicated the introduction of the SO_2-sulfone group in para-ester and triazine ring skeleton vibration in melamine. The absorption peak at 1138 cm^{-1} belonged to the vibration on the sulfonic acid group of SDTES. The absorption peak at 851 cm^{-1} corresponded well to the absorption peak of C-Cl bonds. The absorption peak at 746 cm^{-1} was for the 1,4-bisbenzene substitution. As shown in Figure 3(b), the FTIR spectrum of the para-ester had an absorption peak at 3438 cm^{-1}, which was derived from the N-H stretching vibration of primary amine. The absorption peak at 2922 cm^{-1} was generated by methylene stretching vibration. C-C stretching vibration peaks of benzene ring emerged at 1659 cm^{-1} and 1495 cm^{-1}. The peaks at 1296 cm^{-1} and 1147 cm^{-1} were associated with the SO_2-sulfone and C-O stretching vibration, respectively. And the absorption peak at 825 cm^{-1} can be indexed to the out-of-plane bending vibration of the adjacent hydrogens of the benzene ring. As shown in Figure 3(c), the C-H absorption peak of cyanuric chloride appeared at 3439 cm^{-1}. The absorption peak at 1497 cm^{-1} and 1269 cm^{-1} may be due to the skeletal vibrations of triazine ring. The peak at 848 cm^{-1} was assigned to the absorption of C-Cl bonds. And the peak at 784 cm^{-1} was related to 1,4-bisbenzene [26]. All this indicated the successful preparation of SDTES by the reaction of cyanuric chloride and para-esters.

In Figures 3(d)–3(f), all had the characteristic absorption peak at 3424 cm^{-1}, which was assigned to C=C bonds in CB. For CB/KH550 in Figure 3(e), the absorption bands at 1623 cm^{-1} and 1134 cm^{-1} confirmed the existence of amino and -O-Si- from KH550 [27]. For CB/KH550/SDTES in Figure 3(f), the peaks at 1520 cm^{-1}, 1223 cm^{-1}, and 1154 cm^{-1} were related to the imine, phenyl, and sulfonic acid groups from SDTES, respectively. These groups were in favor of the hydrophilicity of CB, leading to the homodisperse in aqueous situation.

3.3. TEM Analysis. Figure 4 reveals the TEM images of CB and CB/KH550/SDTES. As exhibited in Figure 4(a), CB was granular agglomerated with poor dispersion. The dispersibility was hindered as a result of small particle diameter, large surface area, and strong Van der Waals forces between particles. From Figure 4(b), CB/KH550/SDTES was homogeneously dispersed in the water solution. The existence of sulfonic acid groups on the surface resulted in the static repulsive force between particles. Besides, the enlarged particle size led to enhanced steric hindrance. Therefore, the dispersion of CB/KH550/SDTES was greatly improved.

3.4. Dispersion Stability Analysis. Table 1 displays the particle size, zeta potential, and PDI of CB, CB/KH550, and CB/KH550/SDTES, separately. CB was poorly dispersed in water with particle size of 46.3 nm, zeta potential of -21.10 mV, and PDI of 0.272. The possible reason might be the oxygen groups on the powder surface were inadequate for CB to uniformly disperse in water [28]. The particle size of CB/KH550 was a little larger than that of CB, owing to the presence of amino groups generated by the reaction between KH550 and CB. It was noted that the zeta potential was converted from negative to positive, which was in virtue of the introduction of amino on the CB/KH550 surface. And the absolute value of zeta potential (23.00 mV) suggested CB/

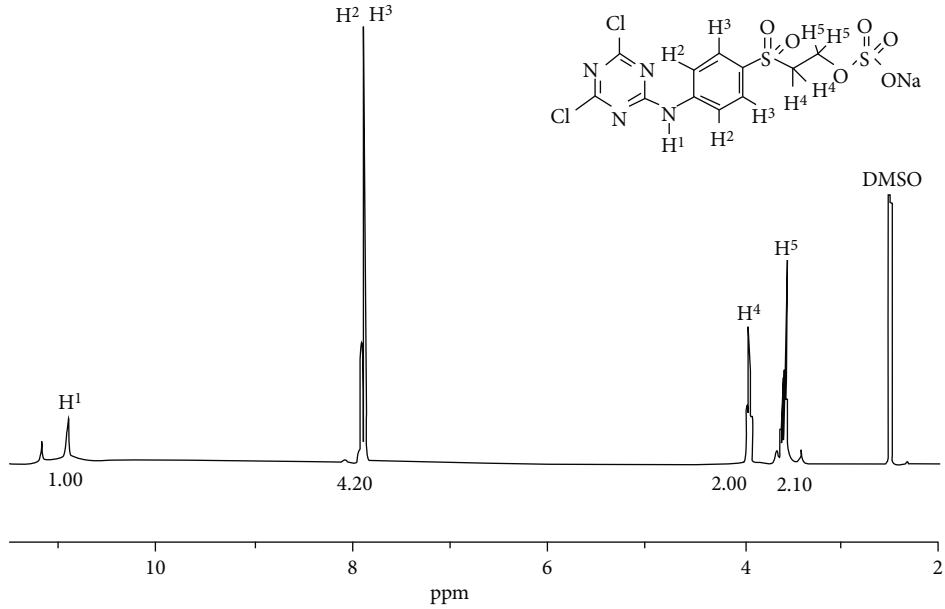

Figure 2: ^{1}H NMR spectrum of SDTES.

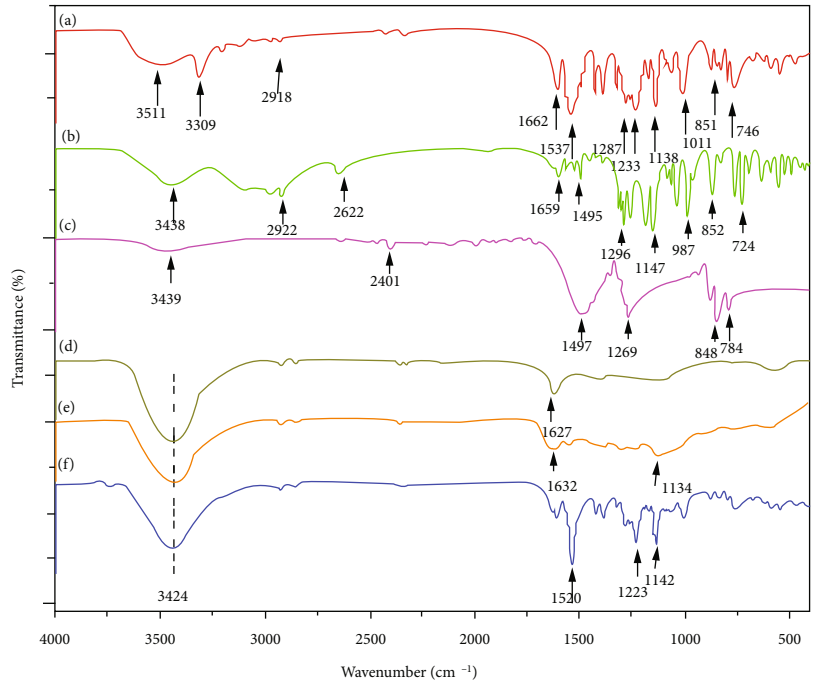

Figure 3: FTIR spectra: (a) SDTES, (b) para-ester, (c) cyanuric chloride, (d) CB, (e) CB/KH550, and (f) CB/KH550/SDTES.

KH550 had better dispersion than CB. The size of CB/KH550/SDTES increased compared to that of CB, which indicated that SDTES was successfully reacted with CB/KH550. And the resulting CB/KH550/SDTES exhibited extraordinary dispersibility. It was worth mentioning that the zeta potential of CB/KH550/SDTES (-38.70 mV) was altered to negative again due to the introduction of the sulfonic acid group, which led to the static repulsive force between the particles. From PDI, it could be speculated that CB/KH550/SDTES ranked the first among all the samples.

Figure 5 exhibits the dispersion stability photos of CB and CB/KH550/SDTES before and after standing for one month. Both samples could form homogeneous dispersion under ultrasonic treatment. After standing for one month,

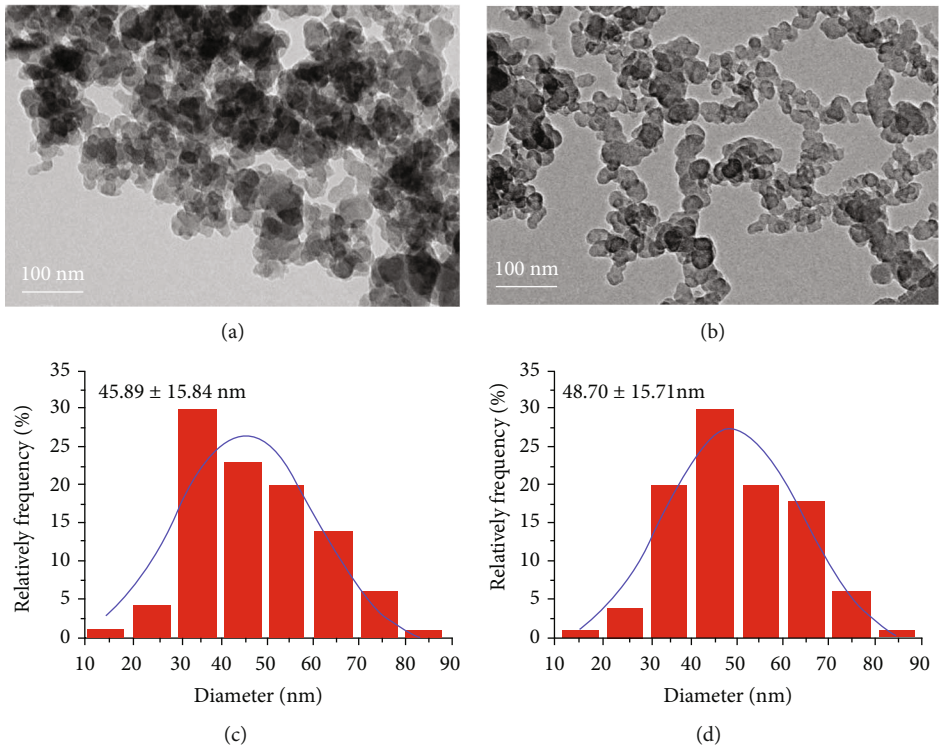

Figure 4: TEM images and diameters: ((a) and (c)) CB and ((b) and (d)) CB/KH550/SDTES.

Table 1: Particle size, zeta potential, and PDI.

Samples	Particle size (nm)	Zeta potential (mV)	PDI
CB	46.3 ± 12.2	−21.10 ± 1.2	0.272 ± 0.2
CB/KH550	47.6 ± 13.5	+23.00 ± 1.4	0.264 ± 0.1
CB/KH550/SDTES	48.9 ± 14.1	−38.70 ± 1.7	0.257 ± 0.1

CB settled at the very bottom of the container, and there was an obvious boundary between the sediment and the supernatant. To the contrary, CB/KH550/SDTES solution remained uniformly dispersed, even after the inversion of the container. All this demonstrated that CB/KH550/SDTES could be stably dispersed in water.

3.5. TG Analysis. Figure 6 illustrates the TG patterns of CB and CB/KH550/SDTES. Both samples showed weight loss at 150°C as a result of water evaporation adsorbed on the surface. It could be observed in Figure 6(a) that CB lost about 2% of its weight and showed insignificant weight loss with the increasing temperature. Low content of moisture adsorbed on the surface may attribute to this phenomenon. However, CB/KH550/SDTES exhibited apparent weight loss of 9.4% on account of the sufficient water content adsorbed on its surface. When the temperature was up to around 320°C and 510°C, the weight loss of CB was almost negligible, while the weight of CB/KH550/SDTES jumped off precipitously owing to thermal decomposition of the KH550 and SDTES, respectively.

3.6. SEM Analysis. Figure 7 shows the SEM images of cotton fabric and cotton fabric dyed with CB/KH550/SDTES. Figures 7(a) and 7(b) showed that the cotton fabric was smooth with natural convolution [29]. And Figures 7(c) and 7(d) clearly showed that the dyed cotton fabric was covered by nanoparticles, which suggested that CB was successfully grafted on the fiber.

3.7. Static Resistance Analysis. Table 2 displays the half-life of electrostatic voltage and specific resistance of cotton fabric. The cotton fabric dyed with CB/KH550/SDTES had better antistatic performance than cotton fabric as the dyed cotton fabric had the shorter half-life of electrostatic voltage (2.5 s) than cotton fabric (8.4 s). CB/KH550/SDTES might play a vital role in endowing antistatic property to the fabric. The R_V and R_S of cotton fabric were $3.82 \times 10^{11}\ \Omega$ – cm and $1.57 \times 10^{14}\ \Omega$, respectively. After being dyed, R_v and R_s were $2.46 \times 10^{10}\ \Omega \cdot$ cm and $2.27 \times 10^{12}\ \Omega$, separately. The R_V and R_S of the cotton fabric were both greater than those of the dyed cotton fabric. All this indicated that the cotton fabric dyed with CB/KH550/SDTES possessed good antistatic effect.

3.8. Ultraviolet Protection Analysis. Table 3 exhibits the ultraviolet protection of cotton fabric. UVA and UVB of cotton fabric were 4.84% and 5.86%, respectively, which were much higher than those of the cotton fabric dyed with CB/KH550/SDTES. This indicated that the ultraviolet was difficult to transmit the dyed cotton fabric. The UPF of the dyed

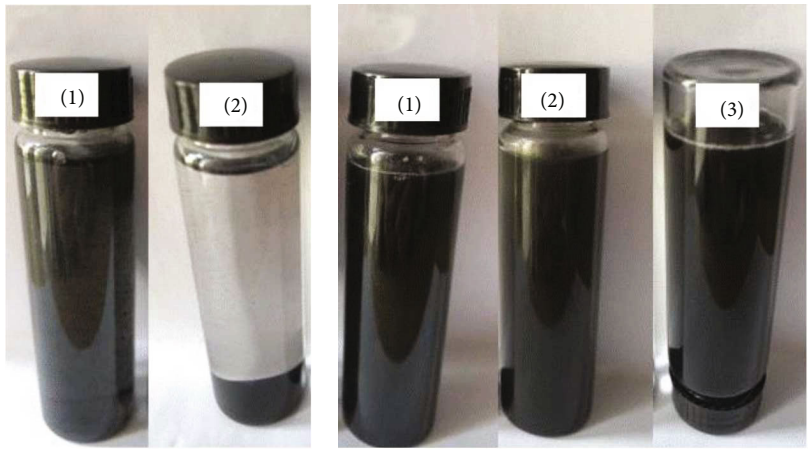

Figure 5: Photos of dispersion stability before and after standing for one month: (a) CB and (b) CB/KH550/SDTES.

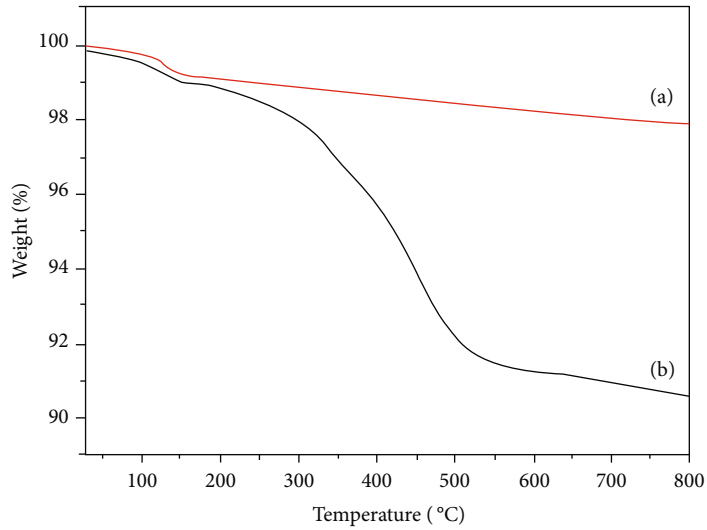

Figure 6: TG patterns: (a) CB and (b) CB/KH550/SDTES.

cotton fabric (57.8) was over three times that of cotton fabric (17.91), which showed that the cotton fabric dyed with CB/KH550/SDTES had preferable ultraviolet resistance.

3.9. Color Depth, Tensile Property, and Rub Fastness Analysis. Table 4 depicts the K/S value, breaking strength and elongation, and rub fastness of cotton fabric. The K/S value (13.81) confirmed the dark appearance of the dyed cotton fabric, which demonstrated that CB/KH550/SDTES was uniformly grafted on the cotton fabric surface.

The dyed cotton fabric (573.6 N) had lower breaking strength than cotton fabric (625.9 N), while the elongation of the dyed cotton fabric (9.69%) was higher than that of cotton fabric (8.86%). The dry and wet rub fastness of the dyed cotton fabric was up to level 4 and level 3, respectively, suggesting an adorable abrasive resistance.

3.10. Mechanism and Reactions for the Binding of CB/KH550/SDTES with Cotton Fabric. The mechanism and reactions for the binding of CB/KH550/SDTES with cotton fabric are proposed in Figure 8. CB/KH550/SDTES with negative charge was achieved by introducing sulfonic groups and chlorine atoms, respectively. Cyanuric chloride (TCT) was selected due to the various activities of three chlorine atoms at different temperature ranges [30–32]. In detail, CB/KH550 was obtained in a reaction between silane coupling agent KH550 and CB with the existence of concentrated ammonia solution. Afterward, SDTES was synthesized by the reaction of one chlorine atom in TCT and the amino group in para-ester at 0°C. Subsequently, CB/KH550/SDTES was prepared by the nucleophile substitution reaction between the amino group in CB/KH550 and one chlorine atom in SDTES at 40°C. Finally, CB/KH550/SDTES was grafted on cotton fabric as a result of the reaction of one chlorine atom in CB/KH550/

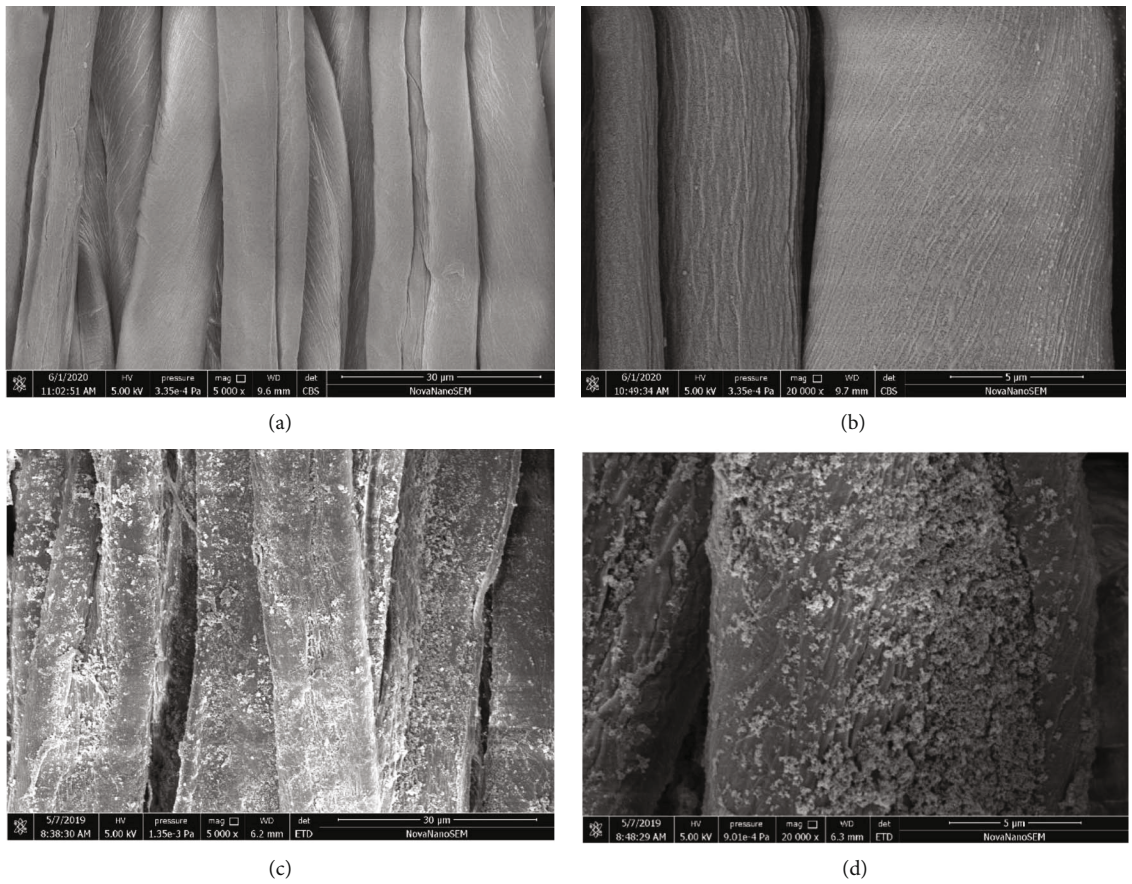

Figure 7: SEM images: (a) cotton fabric (×5,000), (b) cotton fabric (×20,000), (c) cotton fabric dyed with CB/KH550/SDTES (×5,000), and (d) cotton fabric dyed with CB/KH550/SDTES (×20,000).

Table 2: Static resistance and specific resistance.

Samples	$t_{1/2}$ (s)	R_V (Ω·cm)	R_S (Ω)
Cotton fabric	8.4 ± 1.25	$3.82 \pm 0.6 \times 10^{11}$	$1.57 \pm 0.1 \times 10^{14}$
Cotton fabric dyed with CB/KH550/SDTES	2.5 ± 0.8	$2.46 \pm 0.3 \times 10^{10}$	$2.27 \pm 0.1 \times 10^{12}$

Table 3: Ultraviolet protection of cotton fabric.

Samples	UVA (%)	UVB (%)	UPF
Cotton fabric	4.84 ± 0.38	5.86 ± 0.35	17.91 ± 2.25
Cotton fabric dyed with CB/KH550/SDTES	1.93 ± 0.15	2.40 ± 0.13	57.80 ± 5.21

Table 4: Color depth, tensile property, and abrasive resistance of cotton fabric.

Samples	K/S values	Breaking strength (*N*)	Breaking elongation ratio (%)	Dry rub fastness	Wet rub fastness
Cotton fabric	/	625.9 ± 43.9	8.86 ± 0.79	/	/
Cotton fabric dyed with CB/KH550/SDTES	13.81 ± 1.12	573.6 ± 45.8	9.69 ± 0.82	Level 4	Level 3

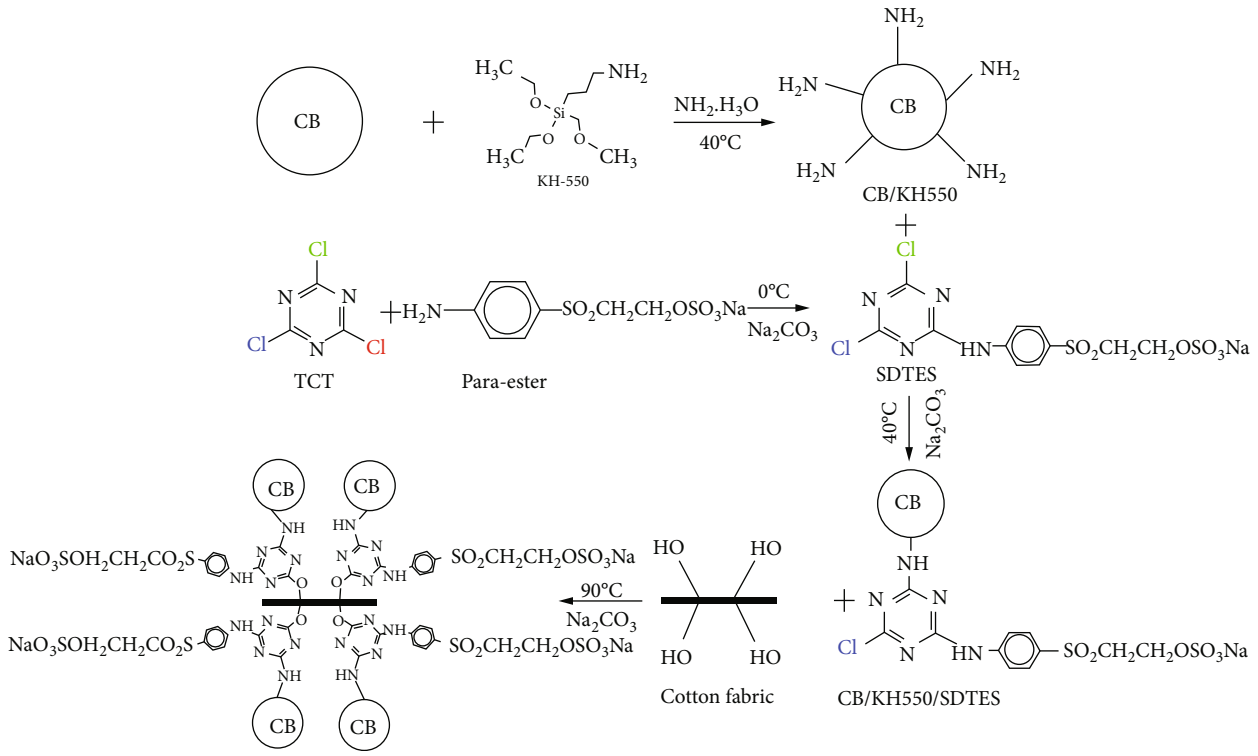

Figure 8: Mechanism and reactions for the binding of CB/KH550/SDTES with cotton fabric.

SDTES and hydroxyl group in cotton fabric under alkaline condition at 90°C [33–35].

4. Conclusions

CB/KH550/SDTES was successfully prepared via three-step chemical reaction and was further grafted onto cotton fabric by dip-dyeing method. Results showed that CB/KH550/SDTES demonstrated excellent dispersibility and storage stability. The cotton fabric dyed with CB/KH550/SDTES exhibited adorable color depth, rub fastness, exceptional ultraviolet protection, and excellent antistatic performance. Besides, the dyed cotton fabric had no obvious decrease in tensile property compared to cotton fabric. The proposed mechanism for the preparation of the cotton fabric dyed with CB may provide a new insight for the dyeing of textiles.

Data Availability

The data used to support the findings of this study are available from the corresponding author upon request.

Conflicts of Interest

There are no conflicts to declare.

References

[1] C. Xu, L. Zhang, D. Xu, M. Li, Y. Zhang, and S. Fu, "Preparation of reactive nanoscale carbon black dispersion for pad coloration of cotton fabric," *Coloration Technology*, vol. 134, no. 2, pp. 91–99, 2018.

[2] D. Li and G. Sun, "Coloration of textiles with self-dispersible carbon black nanoparticles," *Dyes and Pigments*, vol. 72, no. 2, pp. 144–149, 2007.

[3] M. Inagaki, "Carbon coating for enhancing the functionalities of materials," *Carbon*, vol. 50, no. 9, pp. 3247–3266, 2012.

[4] M. H. Abu Elella, E. S. Goda, H. Gamal, S. M. El-Bahy, M. A. Nour, and K. R. Yoon, "Green antimicrobial adsorbent containing grafted xanthan gum/SiO2 nanocomposites for malachite green dye," *International Journal of Biological Macromolecules*, vol. 191, pp. 385–395, 2021.

[5] M. H. Abu Elella, D. H. Hanna, R. R. Mohamed, and M. W. Sabaa, "Synthesis of xanthan gum/trimethyl chitosan interpolyelectrolyte complex as pH-sensitive protein carrier," *Polymer Bulletin*, 2021.

[6] W.-B. Ding, L. Wang, Q. Yang, W.-D. Xiang, J.-M. Gao, and W. A. Amer, "Recent research progress on polymer grafted carbon black and its novel applications," *International Polymer Processing*, vol. 28, no. 2, pp. 132–142, 2013.

[7] C. Wang, X. Zhang, F. Lv, and L. Peng, "Using carbon black nanoparticles to dye the cationic-modified cotton fabrics," *Journal of Applied Polymer Science*, vol. 124, pp. 5194–5199, 2011.

[8] F. Arduini, S. Cinti, V. Mazzaracchio, V. Scognamiglio, A. Amine, and D. Moscone, "Carbon black as an outstanding and affordable nanomaterial for electrochemical (bio)sensor design," *Biosensors and Bioelectronics*, vol. 156, article 112033, 2020.

[9] M. K. Mehrizi, S. M. Mortazavi, S. Mallakpour, S. M. Bidoki, M. Vik, and M. Vikova, "The effect of carbon black nanoparticles on some properties of air plasma printed cotton/polyamide 6 fabrics," *Fibers and Polymers*, vol. 14, no. 10, pp. 1620–1626, 2013.

[10] L. Wang, L. Zhang, D. Wang, M. Li, C. Du, and S. Fu, "Surface modification of carbon black by thiol-ene click reaction for improving dispersibility in aqueous phase," *Journal of Dispersion Science and Technology*, vol. 40, no. 1, pp. 152–160, 2019.

[11] E. S. Goda, M. H. Abu Elella, M. Sohail et al., "N-methylene phosphonic acid chitosan/graphene sheets decorated with silver nanoparticles as green antimicrobial agents," *International Journal of Biological Macromolecules*, vol. 182, pp. 680–688, 2021.

[12] E. S. Goda, M. H. Abu Elella, S. E. Hong, B. Pandit, K. R. Yoon, and H. Gamal, "Smart flame retardant coating containing carboxymethyl chitosan nanoparticles decorated graphene for obtaining multifunctional textiles," *Cellulose*, vol. 28, no. 8, pp. 5087–5105, 2021.

[13] A. H. Keshavarz, M. Mohseni, and M. Montazer, "Electro-conductive modification of polyethylene terephthalate fabric with nano carbon black and washing fastness improvement by dopamine self-polymerized layer," *Journal of Applied Polymer Science*, vol. 136, no. 41, article 48035, 2019.

[14] M. H. Abu Elella, M. W. Sabaa, D. H. Hanna, M. M. Abdel-Aziz, and R. R. Mohamed, "Antimicrobial pH-sensitive protein carrier based on modified xanthan gum," *Journal of Drug Delivery Science and Technology*, vol. 57, article 101673, 2020.

[15] M. H. Abu Elella, E. S. Goda, K. R. Yoon et al., "Novel vapor polymerization for integrating flame retardant textile with multifunctional properties," *Composites Communications*, vol. 24, article 100614, 2021.

[16] S. Trostová, I. Stibor, J. Karpíšková, Z. Kolská, and V. Švorčík, "Characterization of surface chemical modified carbon nanoparticles," *Materials Letters*, vol. 102-103, pp. 83–86, 2013.

[17] M. Atif, R. Bongiovanni, M. Giorcelli, E. Celasco, and A. Tagliaferro, "Modification and characterization of carbon black with mercaptopropyltrimethoxysilane," *Applied Surface Science*, vol. 286, pp. 142–148, 2013.

[18] M. Zhou, K. Huang, D. Yang, and X. Qiu, "Development and evaluation of polycarboxylic acid hyper-dispersant used to prepare high-concentrated coal–water slurry," *Powder Technology*, vol. 229, pp. 185–190, 2012.

[19] M. M. Abdel-Aziz, M. H. A. Elella, and R. R. Mohamed, "Green synthesis of quaternized chitosan/silver nanocomposites for targeting _mycobacterium tuberculosis_ and lung carcinoma cells (A-549)," *International Journal of Biological Macromolecules*, vol. 142, pp. 244–253, 2020.

[20] M. H. Abu Elella, E. S. Goda, M. A. Gab-Allah et al., "Xanthan gum-derived materials for applications in environment and eco-friendly materials: a review," *Journal of Environmental Chemical Engineering*, vol. 9, no. 1, article 104702, 2021.

[21] P. Xue, J. Gao, Y. Bao, J. Wang, Q. Li, and C. Wu, "An analysis of microstructural variations in carbon black modified by oxidation or ultrasound," *Carbon*, vol. 49, no. 10, pp. 3346–3355, 2011.

[22] Y. Li, W. Zhang, J. Zhao et al., "A route of alkylated carbon black with hydrophobicity, high dispersibility and efficient thermal conductivity," *Applied Surface Science*, vol. 538, article 147858, 2021.

[23] Q. Jiang, S. Wang, and S. Xu, "Preparation and characterization of water-dispersible carbon black grafted with polyacrylic acid by high-energy electron beam irradiation," *Journal of Materials Science*, vol. 53, no. 8, pp. 6106–6115, 2018.

[24] A. Tian, L. Zhang, C. Wang, S. Fu, and C. Xu, "Preparation of SiO2/PSSS dispersion for formulation of white inkjet ink," *Polymer Bulletin*, vol. 72, no. 5, pp. 963–975, 2015.

[25] J. Akrman and J. Přikryl, "Application of benzotriazole reactive UV absorbers to cellulose and determining sun protection of treated fabric spectrophotometrically," *Journal of Applied Polymer Science*, vol. 108, no. 1, pp. 334–341, 2008.

[26] M. Prabhaharan, A. R. Prabakaran, S. Srinivasan, and S. Gunasekaran, "Experimental and theoretical spectroscopic analysis, HOMO–LUMO, and NBO studies of cyanuric chloride," *Spectrochimica Acta Part A: Molecular and Biomolecular Spectroscopy*, vol. 127, pp. 454–462, 2014.

[27] M. Wei, S. Wang, C. Sun, C. Zhou, and J. Ni, "Modification and characterization of nano-TiO2 for efficient fixation on cotton fibers," *Fibers and Polymers*, vol. 19, no. 11, pp. 2278–2283, 2018.

[28] L. Wang, L. Zhang, Y. Zhang, M. Li, and S. Fu, "Preparation and characterization of aqueous phase self-dispersed CB/PSSS composites," *Colloids and Surfaces A: Physicochemical and Engineering Aspects*, vol. 533, pp. 33–40, 2017.

[29] Z. Qi, K. Wang, Y. Jiang et al., "Preparation and characterization of SnO2−x/GO composite photocatalyst and its visible light photocatalytic activity for self-cleaning cotton fabrics," *Cellulose*, vol. 26, no. 16, pp. 8919–8937, 2019.

[30] R. Ma, M. Zhao, Y. Mo, P. Tang, Y. Feng, and D. Li, "HALS intercalated layered double hydroxides as an efficient light stabilizer for polypropylene," *Applied Clay Science*, vol. 180, article 105196, 2019.

[31] A. El-Faham, S. M. Soliman, S. M. Osman et al., "One pot synthesis, molecular structure and spectroscopic studies (X-ray, IR, NMR, UV–Vis) of novel 2-(4,6-dimethoxy-1,3,5-triazin-2-yl) amino acid ester derivatives," *Spectrochimica Acta Part A: Molecular and Biomolecular Spectroscopy*, vol. 159, pp. 184–198, 2016.

[32] M. Soltani Rad, A. Khalafi-Nezhad, Z. Asrari, and S. Behrouz, "Highly efficient one-pot synthesis of N-acylsulfonamides using cyanuric chloride at room temperature," *Synthesis*, vol. 2010, no. 15, pp. 2599–2603, 2010.

[33] Z. Jiang, K. Ma, J. Du, R. Li, X. Ren, and T. S. Huang, "Synthesis of novel reactive N-halamine precursors and application in antimicrobial cellulose," *Applied Surface Science*, vol. 288, pp. 518–523, 2014.

[34] M. Zhang, Y. Zhang, Y. Liu, X. Ren, and T. Huang, "Simultaneous low-alt dyeing and anti-bacterial finishing of cotton fabric with reactive dye and N-halamine," *Coloration Technology*, vol. 137, no. 5, pp. 475–483, 2021.

[35] Z. M. Qi, K. Wang, J. Y. Chen, D. W. Gao, Y. Ren, and C. X. Wang, "Cotton fabric loaded with self-dispersive and reactive biphasic TiO_2 for durable self-cleaning activity and ultraviolet protection," *New Journal of Chemistry*, vol. 45, no. 25, pp. 11119–11129, 2021.